4568 *Chem. Mater.* **2009,** *21,* 4568–4576
DOI:10.1021/cm9015113

CHEMISTRY OF MATERIALS
Article

Understanding the p-Type Conduction Properties of the Transparent Conducting Oxide $CuBO_2$: A Density Functional Theory Analysis

David O. Scanlon,*,† Aron Walsh,‡ and Graeme W. Watson*,†

†*School of Chemistry, Trinity College Dublin, Dublin 2, Ireland, and* ‡*Department of Chemistry, University College London, 20 Gordon Street, London WC1H 0AJ, U.K.*

Received June 2, 2009. Revised Manuscript Received July 30, 2009

Discovering new candidate p-type transparent conducting oxides has become a major goal for material scientists. Recently delafossite $CuBO_2$ has been proposed as a promising candidate, showing good room temperature electrical conductivity and excellent transparency [*Appl. Phys. Lett.* **2007**, *91*, 092123]. In this article we report a density functional theory investigation of $CuBO_2$, examining the geometry and electronic structure using GGA corrected for on-site Coulomb interactions (GGA + *U*) and a hybrid density functional (HSE06). From analysis of the calculated band structure, density of states, and optical absorption, we predict an indirect fundamental band gap of ∼3.1 eV and a direct optical band gap of ∼3.6 eV. The hole effective mass at the valence band maximum indicates the potential for good p-type conductivity, consistent with the reported experimental results. These results are discussed in relation to other delafossite oxides.

Introduction

Transparent conducting oxides (TCOs) are unique materials that combine concomitant electrical conductivity and optical transparency in a single material, possessing carrier concentrations of at least 10^{20} cm^{-3} and optical band gaps greater than 3 eV.[1] This appealing combination of conductivity and transparency make TCOs valuable technological materials, which are currently utilized in a number of commercial applications.[2] Development of functional p−n junctions solely using TCO materials is a major goal for material scientists, as this would open up the possibility of "Transparent Electronics".[3] This goal necessitates the production of good quality n- and p-type TCO materials.

While high performance n-type TCOs (SnO_2,[4] In_2O_3,[5] and ZnO[6]) have become standard,[7] p-type TCOs have proved harder to develop. The top of the valence band of most wide band gap binary oxides is usually dominated by O 2p states, which when doped p-type, results in deep lying, strongly localized O 2p holes, limiting any electronic conduction.[8] For decades research had been focused on doping the usually n-type TCO materials to make them p-type, and indeed this research is still ongoing in the case of ZnO.[9,10]

In 1997, Kawazoe et al. first reported p-type conductivity and transparency in thin films of $CuAlO_2$.[11] Subsequently, Hosono and co-workers postulated that combining the valence band features of Cu_2O (a native p-type oxide with an optical band gap of ∼2.17 eV which precludes it as a TCO[12]) with the larger band gaps of other binary oxides was an appealing method of developing p-type TCOs.[13] In Cu_2O, the Cu occupied 3d states hybridize with the O 2p states in the valence band (VB), with Cu d states dominating at the top of the VB.[12] Thus, upon hole formation (due to oxygen excess), $3d^{10}$ Cu(I) is oxidized to $3d^9$ Cu(II),[12] creating holes on Cu ions. As the Cu states are hybridized with oxygen, this leads to *less* localized holes with *increased* mobility. These valence band features are still present in $CuAlO_2$, meaning $CuAlO_2$ retains the p-type features of Cu_2O,[11] and this has been evidenced in many previous theoretical and experimental studies on the electronic structure of Cu(I)-based Delafosites.[14−16]

*Corresponding authors. E-mail: scanloda@tcd.ie; watsong@tcd.ie.

(1) Gordon, R. G. *MRS Bull.* **2000**, *25*, 52–57.
(2) Banerjee, A. N.; Chattopadhyay, K. K. *Prog. Cryst. Growth Charact. Mater.* **2005**, *50*, 52.
(3) Thomas, G. *Nature* **1997**, *389*, 907.
(4) Godinho, K. G.; Walsh, A.; Watson, G. W. *J. Phys. Chem. C* **2008**, *113*, 439–448.
(5) Walsh, A.; Da Silva, J. L. F.; Wei, S. H.; Korber, C.; Klein, A.; Piper, L. F. J.; DeMasi, A.; Smith, K. E.; Panaccione, G.; Torelli, P.; Payne, D. J.; Bourlange, A.; Egdell, R. G. *Phys. Rev. Lett.* **2008**, *100*, 167402.
(6) Kohan, A. F.; Ceder, G.; Morgan, D.; Van de Walle, C. G. *Phys. Rev. B* **2000**, *61*, 15019–15027.
(7) Minami, T. *Semicond. Sci. Technol.* **2005**, *20*, S35–S44.
(8) Schirmer, O. F. *J. Phys.: Condens. Matter* **2006**, *18*, R667–R704.
(9) Li, J.; Wei, S. H.; Li, S. S.; Xia, J. B. *Phys. Rev. B* **2006**, *74*, 081201.
(10) Yan, J. B.; Li, Y. F.; Wei, S. H.; Al-Jassim, M. M. *Phys. Rev. Lett.* **2007**, *98*, 135506.
(11) Kawazoe, H.; Yasakuwa, H.; Hyodo, H.; Kurita, M.; Yanagi, H.; Hosono, H. *Nature* **1997**, *389*, 939.
(12) Hu, J. P.; Payne, D. J.; Egdell, R. G.; Glans, P. A.; Learmonth, T.; Smith, K. E.; Guo, J.; Harrison, N. M. *Phys. Rev. B* **2008**, *77*, 155115.
(13) Kawazoe, H.; Yanagi, H.; Ueda, K.; Hosono, H. *MRS Bull.* **2000**, *25*, 28–36.
(14) Buljan, A.; Alemany, P.; Ruiz, E. *J. Phys. Chem. B* **1999**, *103*, 8060–8066.
(15) Kandpal, H. C.; Seshadri, R. *Solid State Sci.* **2002**, *4*, 1045–1052.
(16) Aston, D. J.; Payne, D. J.; Green, A. J. H.; Egdell, R. G.; Law, D. S. L.; GuO, J.; Gland, P. A.; Learmonth, T.; Smith, K. E. *Phys. Rev. B* **2005**, *72*, 195115.

 Published on Web 09/02/2009

The relatively small band gap of Cu_2O is thought to be caused by the three-dimensional interactions between the $3d^{10}$ electrons on neighboring Cu(I) ions.[17] These three-dimensional interactions arise due to the structure of the system, which can be thought of as being made up of two interpenetrating cristobalite lattices.[18,19] In the delafossite structure (Figure 1) each Cu atom is linearly coordinated with two oxygen atoms, forming O−Cu−O dumbbells parallel to the *c* axis. Oxygens in these O−Cu−O units are also each coordinated to three M(III) atoms, oriented such that M(III)-centered octahedra form $M(III)O_2$ layers which lie parallel to the *ab* plane. Two alternative layer stackings are possible, resulting in a hexagonal (space group *P*63/*mmc*) or rhombohedral (space group *R*3-*mh*) unit cell.[20] Thus, the delafossite structure decreases the dimensionality of the Cu−Cu interactions, usually resulting in band gaps large enough for TCO applications.[21] These theories were confirmed by the extensive theoretical work of Alemany and co-workers.[22,23]

Since the discovery of p-type conductivity in $CuAlO_2$, many Cu(I) based delafossites having transparency and p-type conductivity have been synthesized, including $CuScO_2$, $CuYO_2$, $CuInO_2$, $CuGaO_2$, and $CuCrO_2$.[24] Indeed, other structures have been identified that combine p-type conductivity and optical transparency in Cu(I) based materials, including $SrCu_2O_2$[25,26] and layered oxychalogenides (LaCuOS),[27] although to date the p-type TCO with the highest conductivity is a delafossite (Mg doped $CuCrO_2$).[28]

Until 2002, the behavior of the group 13 (group IIIA) delafossites (Al, Ga, In) was not well understood, with apparent band gap anomalies and the issue of bipolar doping proving very puzzling.[11,17,29,30] Group 13 semiconductors are known to have direct band gaps that decrease as the atomic number of the group 13 element increases,[31] for example, $CuMS_2$ and MAs (M = Al, Ga, In). In group 13 delafossites the trend was thought to be reversed, with optically measured bandgaps that increased as the atomic number increased going down the group.[11,17,29,30] Wei and co-workers used first principles methods to investigate the electronic structure of these materials, showing that these materials did obey the trends seen in other group 13 containing semiconductors.[32] They found using LDA that *both* the calculated indirect band gap and direct band gaps *do* decrease as the

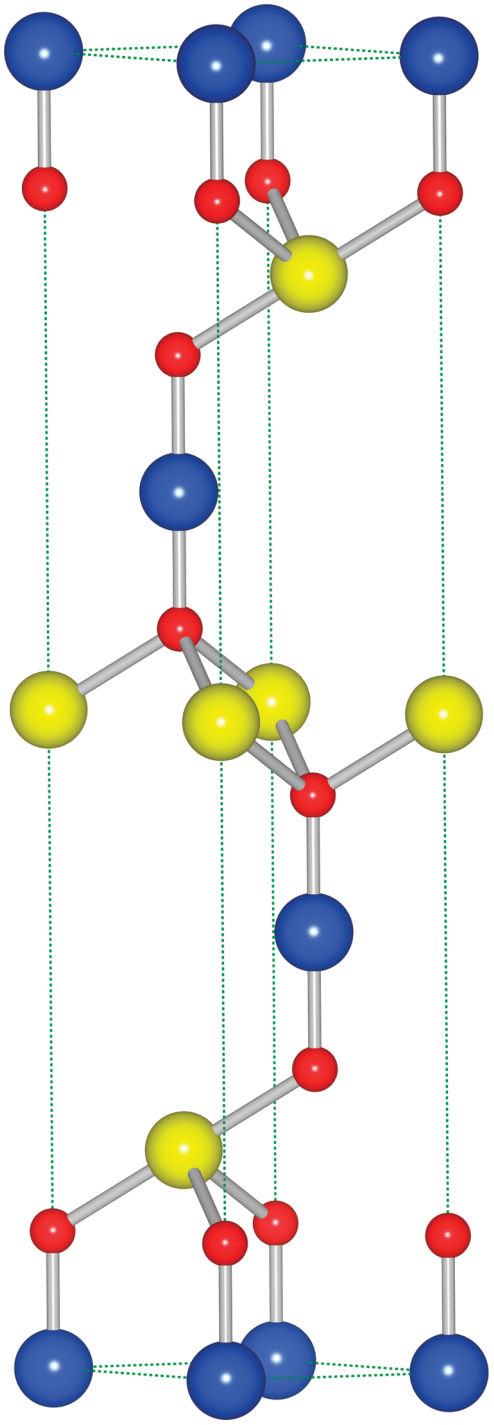

Figure 1. Conventional unit cell of rhombohedral $CuBO_2$. The red, blue, and yellow balls are oxygen, copper, and boron respectively.

(17) Yanagi, H.; Inoue, S.; Ueda, K.; Kawazoe, H.; Hosono, H.; Hamada, N. *J. Appl. Phys.* **2000**, *88*, 4059–4163.
(18) Onsten, A.; Månsson, M.; Claesson, T.; Muro, T.; Matsushita, T.; Nakamura, T.; Kinoshita, T.; Karlsson, U. O.; Tjernberg, O. *Phys. Rev. B* **2007**, *76*, 115127.
(19) Laskowski, R.; Blaha, P.; Schwarz, K. *Phys. Rev. B* **2003**, *67*, 075102.
(20) Köhler, B. U.; Jansen, M. *Z. Anorg. Allg. Chem.* **1986**, *543*, 73.
(21) Filippetti, A.; Fiorentini, V. *Phys. Rev. B* **2005**, *72*, 035128.
(22) Ruiz, E.; Alvarez, S.; Alemany, A.; Evarestov, R. *Phys. Rev. B* **1997**, *56*, 7189.
(23) Buljan, A.; Llunell, M.; Ruiz, E.; Alemany, P. *Chem. Mater.* **2001**, *13*, 338–344.
(24) Marquardt, M. A.; Ashmore, N. A.; Cann, D. P. *Thin Solid Films* **2006**, *496*, 146–156.
(25) Kudo, A.; Yanagi, H.; Hosono, H.; Kawazoe, H. *Appl. Phys. Lett.* **1998**, *73*, 220–222.
(26) Godinho, K. G.; Watson, G. W.; Walsh, A.; Green, A. J. H.; Payne, D. J.; Harmer, J.; Egdell, R. G. *J. Mater. Chem.* **2008**, *18*, 2798–2806.
(27) Ueda, K.; Inoue, S.; Hirose, S.; Kawazoe, H.; Hosono, H. *Appl. Phys. Lett.* **2000**, *77*, 2701–2703.
(28) Nagarajan, R.; Draeseke, A. D.; Sleight, A. W.; Tate, J. *J. Appl. Phys.* **2001**, *89*, 8022.
(29) Ueda, K.; Hase, t.; Yanagi, H.; Kawazoe, H.; Hosono, H.; Ohta, H.; Orita, M.; Hirano, M. *J. Appl. Phys.* **2001**, *89*, 1790.
(30) Yanagi, H.; Hase, T.; Ibuki, S.; Ueda, k.; Hosono, H. *Appl. Phys. Lett.* **2001**, *78*, 1583.
(31) *Landolt-Bornstein: Numerical Data and Functional Relationships in Science and technology*; Madelung, O., Schulz, M., Eds.; Springer-Verlag: Berlin, 1987; Vol. *22a*.
(32) Nie, X.; Wei, S. H.; Zhang, S. B. *Phys. Rev. Lett.* **2002**, *88*, 066405.

atomic number increases.[32] The optically measured band gap anomalies were thus explained by examining the calculated absorption spectra, which showed trends in keeping with experiment, with the optical band gap *increasing* with increasing atomic number, due to direct transitions at Γ being symmetry disallowed.[32]

Recently, a study by Snure and Tiwari has identified a new group 13 delafossite, $CuBO_2$, as a new p-type TCO.[33] Thin films of $CuBO_2$ display a remarkable room temperature electrical conductivity of 1.65 S cm^{-1},[33] which is, to the best of our knowledge, the highest intrinsic conductivity reported of all the delafosites. A fit to their optical absorption data produces an indirect band gap of 2.2 eV and a direct optical band gap of 4.5 eV. The *a* and *c* lattice vectors have been reported as 2.84 Å and 16.52 Å, respectively, on the basis of X-ray diffraction (XRD) of the films, although the thin film nature may affect these properties.

In this study we present a density functional theory (DFT) study, examining the detailed electronic structure of $CuBO_2$. We show conclusively that (i) the lattice parameters reported by Snure and Tiwari[33] are not consistent with previous experimental trends and need to be reinvestigated, (ii) the valence band features of $CuBO_2$ are consistent with other delafossite p-type TCOs, (iii) the effective hole masses of the valence band maximum (VBM) are consistent with the reported good conductivity, and (iv) the predicted indirect band gap and optical band gap of $CuBO_2$ are 3.21 eV and ~5.1 eV, respectively. The reason for the enhanced conductivity is discussed in relation to other delafossite TCOs.

Calculation Methodology

The periodic DFT code VASP[34,35] was employed for all our calculations, in which a plane wave basis set describes the valence electronic states. In all our calculations, the Perdew−Burke−Ernzerhof[36] (PBE) gradient corrected functional was used to treat the exchange and correlation. Interactions between the cores (Cu:[Ar], B[He], and O:[He]) and the valence electrons were described using the projector-augmented wave[37,38] (PAW) method. Calculations were performed using DFT corrected for on-site Coulombic interactions GGA + U[39] and a hybrid density functional (HSE06)[40] to overcome the errors associated with the DFT self-interaction error (SIE).[41] Cu_2O and Cu(I)-based delafossites, although formaly closed shell systems, are strongly correlated materials, and as such are affected by the SIE. In the case of Cu_2O, the SIE destabilizes the position of the main Cu 3d peak by as much a 1 eV, resulting in excessive hybridization with the O 2p states. Applying a U correction to the *d* states can regain the correct positioning of the Cu 3d peak relative to XPS studies.[12,42] The value of U used in this study was 5.2 eV, which has recently been shown to reproduce the valence band features of Cu_2O, $CuAlO_2$,[43] and $CuCrO_2$[44] from comparison with high resolution XPS spectra. The validity of the GGA + U approach has been demonstrated in its recent use to provide improved descriptions of a wide range of systems including other closed shell systems (e.g., ZnO[45]) and localized electronic defect systems including n-type[46−50] and p-type polarons.[51,52]

Structural optimizations of bulk $CuBO_2$ were performed using GGA + U at a series of volumes to calculate the equilibrium lattice parameters. In each case the atomic positions, lattice vector, and cell angle were allowed to relax, while the total volume was held constant. The resulting energy volume curves were fitted to the Murnaghan equation of state to obtain the equilibrium bulk cell volume.[53] This approach avoids the problems of Pulay stress and changes in basis set which can accompany volume changes in plane wave calculations. Convergence with respect to *k*-point sampling and plane wave energy cut off was checked, and for both systems a cutoff of 500 eV and a *k*-point sampling of 10 × 10 × 10 were found to be sufficient. Calculations were deemed to be converged when the forces on all the atoms were less than 0.001 eV $Å^{-1}$.

While GGA + U provides a definite improvement over generalized gradient approximation/local denisty approximation (GGA/LDA) descriptions of polaronic or strongly correlated systems, it still underestimates the band gap, unless excessively large and unjustifiable values of U are used, leading to poor crystal properties of pure or defective systems relative to experiment.[54] Hybrid functionals, which include a certain percentage of exact Fock exchange, can often give better approximations of band gaps in semiconductor systems and improved structural data.[55] Unfortunately hybrid functionals are very

(33) Snure, M.; Tiwari, A. *Appl. Phys. Lett.* **2007**, *91*, 092123.
(34) Kresse, G.; Hafner, J. *Phys. Rev. B* **1994**, *49*, 14251–14271.
(35) Kresse, G.; Furthmüller, J. *Phys. Rev. B* **1996**, *54*, 11169–11186.
(36) Perdew, J. P.; Burke, K.; Ernzerhof, M. *Phys. Rev. Lett.* **1996**, *77*, 3865.
(37) Blöchl, P. E. *Phys. Rev. B* **1994**, *50*, 17953.
(38) Kresse, G.; Joubert, D. *Phys. Rev. B* **1999**, *59*, 1758–1775.
(39) Dudarev, S. L.; Botton, G. A.; Savrasov, S. Y.; Humphreys, C. J.; Sutton, A. P. *Phys. Rev. B* **1998**, *57*, 1505.
(40) Heyd, S.; Scuseria, G. E.; Ernzerhof, M. *J. Chem. Phys.* **2003**, *118*, 8207–8215.
(41) Morgan, B. J.; Scanlon, D. O.; Watson, G. W. *e-J. Surf. Sci. Nanotechnol.* **2009**, *7*, 395–404.
(42) Raebiger, H.; Lany, S.; Zunger, A. *Phys. Rev. B* **2007**, *76*, 045209.
(43) Scanlon, D. O.; Walsh, A.; Morgan, B. J.; Watson, G. W.; Payne, D. J.; Egdell, R. G. *Phys. Rev. B* **2009**, *79*, 035101.
(44) Arnold, T.; Payne, D. J.; Bourlange, A.; Hu, J. P.; Egdell, R. G.; Piper, L. F. J.; Colakerol, L.; De Masi, A.; Glans, P.-A.; Learmonth, T.; Smith, K. E.; Guo, J.; Scanlon, D. O.; Walsh, A.; Morgan, B. J.; Watson, G. W. *Phys. Rev. B* **2009**, *79*, 075102.
(45) Zhou, G. C.; Sun, L. Z.; Wang, J. B.; Zhong, Z. L.; Zhou, Y. C. *Phys. B: Condens. Matter* **2008**, *403*, 2832–2837.
(46) Morgan, B. J.; Watson, G. W. *Surf. Sci.* **2007**, *601*, 5034–5041.
(47) Scanlon, D. O.; Walsh, A.; Morgan, B. J.; Watson, G. W. *J. Phys. Chem. C* **2008**, *112*, 9903–9911.
(48) Coquet, R.; Willock, D. J. *Phys. Chem. Chem. Phys.* **2005**, *7*, 3819–3828.
(49) Walsh, A.; Yan, Y.; Al-Jassim, M. M.; Wei, S. H. *J. Phys. Chem. C* **2008**, *125*, 12044–12050.
(50) Morgan, B. J.; Scanlon, D. O.; Watson, G. W. *J. Mater. Chem.* **2009**, *19*, 5175–5178.
(51) Nolan, M.; Watson, G. W. *J. Chem. Phys.* **2006**, *125*, 144701–144706.
(52) Scanlon, D. O.; Walsh, A.; Morgan, B. J.; Nolan, M.; Fearon, J.; Watson, G. W. *J. Phys. Chem. C* **2007**, *111*, 7971–7979.
(53) Murnaghan, F. D. *Proc. Natl. Acad. Sci. U.S.A.* **1944**, *30*, 244–247.
(54) Laubach, S.; Schmidt, P. C.; Thissen, A.; Fernandez-Madrigal, F. J.; Wu, Q. H.; Jaegermann, W.; Klemm, M.; Horn, S. *Phys. Chem. Chem. Phys.* **2007**, *9*, 2564–2576.
(55) Labat, F.; Baranek, P.; Domain, C.; Minot, C.; Adamo, C. *J. Chem. Phys.* **2007**, *126*, 154703.

computationally demanding within a plane wave basis set and have in some cases been overlooked in favor of less computationally expensive methods, such as the "+ U" correction, or even a range of a posteriori corrections to LDA/GGA calculations.[42]

In this study we have used the screened hybrid density functional developed by Heyd, Scuzeria, and Ernzerhof (HSE06),[40] as implemented in the VASP code.[56] Difficulties in evaluating the Fock exchange in a real space formalism are caused by the slow decay of the exchange interaction with distance. In the HSE06 hybrid functional approach, this problem is addressed by separating the description of the exchange interaction into long- and a short-range parts.[40] Thus, a percentage ($\alpha = 25\%$) of exact nonlocal Fock exchange is added to the PBE functional (the choice of α is empirical and can vary from system to system,[57] similar to the choice of U in the GGA + U approach), and a screening of $\omega = 0.11$ bohr^{-1} is applied to partition the Coulomb potential into long-range (LR) and short-range (SR) terms. Thus the exchange and correlation terms are

$$E_{xc}^{\mathrm{HSE06}}(\omega) = E_x^{\mathrm{HSE06,\,SR}} + E_x^{\mathrm{PBE,\,LR}} + E_c^{\mathrm{PBE}} \qquad (1)$$

where

$$E_x^{\mathrm{HSE06,\,SR}} = \frac{1}{4}E_x^{\mathrm{Fock,\,SR}} + \frac{3}{4}E_x^{\mathrm{PBE,\,SR}} \qquad (2)$$

Hartree−Fock and PBE exchange are therefore only mixed in the SR part, with the LR exchange interactions being represented by the corresponding part of the range separated PBE functional.[40] HSE06 has been shown to produce structural data and band gap descriptions that are more accurate than LDA/GGA and meta-GGA data.[58−62] For the HSE06 calculations, a cutoff of 400 eV and a k-point sampling of $10 \times 10 \times 10$ were found to be sufficient, and the structure was deemed to be converged when the forces on all the atoms were less than 0.001 eV Å^{-1}.

Both the optical transition matrix elements and the optical absorption spectrum were calculated within the transversal approximation and PAW method.[63] In this approach, the optical transition matrix elements, $\langle\psi_i|\hat{\mathrm{P}}_\alpha|\psi_f\rangle$, between states i and f (with $\hat{\mathrm{P}}_\alpha$ being the momentum operator with polarization α and the PAW all electron wave function denoted ψ), are calculated using the method devised by Adolph et al.[64] The imaginary part of the dielectric function can be derived from the transition matrix elements using:

$$\mathrm{Im}\ \varepsilon_{\alpha\beta}(\omega) = \left(\frac{2\pi e}{m\omega}\right)^2 \sum_{if}\int \mathrm{d}(\mathbf{k})\langle\psi_i|\hat{\mathrm{P}}_\alpha|\psi_f\rangle\langle\psi_f|\hat{\mathrm{P}}_\beta|\psi_i\rangle\delta(E_f(\mathbf{k}) - E_i(\mathbf{k}) - \hbar\omega) \qquad (3)$$

with the integration performed using the tetrahedron method[65] and a fine k-point mesh (in our calculations $10 \times 10 \times 10$ is a sufficiently fine mesh). The real part of the dielectric function, Re $\varepsilon_{\alpha\beta}(\omega)$, can be obtained from the imaginary part using the Kramers−Kronig relations.[66] The absorption coefficient is then calculated using

$$A_{\alpha\alpha}(\omega) = \frac{\sqrt{2[|\varepsilon_{\alpha\alpha}(\omega)| - \mathrm{Re}\ \varepsilon_{\alpha\alpha}(\omega)]}}{c} \qquad (4)$$

In this methodology, the adsorption spectra is summed over all direct VB to conduction band (CB) transitions and therefore ignores indirect and intraband adsorptions.[64] Within this framework of single particle transitions, the electron−hole correlations are not treated and so would require treatment by higher order electronic structure methods.[67,68] Nevertheless, this method has been previously shown to provide reasonable optical absorption spectra.[32,61,69] Structure and charge density visualization and analysis were performed using VESTA.[70]

Results

To the best of our knowledge, there have been no complete crystallographic structural data reported for $CuBO_2$. The only reported estimation of the lattice constants of $CuBO_2$ are reported for thin films of $CuBO_2$, taken from the study undertaken by Snure and Tiwari.[33] Therefore we have adopted two approaches to find the minimum GGA structure for $CuBO_2$: (a) perform a constant volume structural optimization from the estimated lattice constants taken from Snure and Tiwari's study[33] and (b) perform a constant volume structural optimization from a known delafossite structure, closest in magnitude to the proposed structure, which in this case is $CuAlO_2$.

Approaches (a) and (b) both converged to the same structure and produced the calculated structural data shown in Tables 1 and 2. It is clear that the a lattice vectors obtained from our GGA + U calculations (2.53 Å) are significantly smaller than those obtained experimentally for the $CuBO_2$ thin films (2.84 Å).

(56) Paier, J.; Marsman, M.; Hummer, K.; Kresse, G.; Gerber, I. C.; Ángyán, J. G. *J. Chem. Phys.* **2006**, *124*, 154709–154713.
(57) Walsh, A.; Da Silva, J. L. F.; Wei, S. H. *Phys. Rev. Lett.* **2008**, *100*, 256401.
(58) Heyd, J.; Scuseria, G. E. *J. Chem. Phys.* **2004**, *121*, 1187–1192.
(59) Heyd, J.; Peralta, J. E.; Scuseria, G. E.; Martin, R. L. *J. Chem. Phys.* **2005**, *123*, 174101.
(60) Da Silva, J. L. F.; Ganduglia-Pirovano, M. V.; Sauer, J.; Bayer, V.; Kresse, G. *Phys. Rev. B* **2007**, *75*, 045121.
(61) Walsh, A.; Da Silva, J. L. F.; Yan, Y.; Al-Jassim, M. M.; Wei, S. H. *Phys. Rev. B* **2009**, *79*, 073105.
(62) Chen, S.; Gong, Z. G.; Walsh, A.; Wei, S. H. *Appl. Phys. Lett.* **2009**, *94*, 041903.
(63) Gajdos, M.; Hummer, K.; Kresse, G.; Furthmuller, J.; Bechstedt, F. *Phys. Rev. B* **2006**, *73*, 045112.
(64) Adolph, B.; Furthmuller, J.; Beckstedt, F. *Phys. Rev. B* **2001**, *63*, 125108.
(65) Blöchl, P. E.; Jepsen, O.; Andersen, O. K. *Phys. Rev. B* **1994**, *49*, 16223–16233.
(66) Yu, P. Y.; Cardona, M. *Fundamentals of Semiconductors*, 2nd ed.; Springer: New York, 1999.
(67) Ramos, L. E.; Paier, J.; Kresse, G.; Bechstedt, F. *Phys. Rev. B* **2008**, *78*, 195423.
(68) Paier, J.; Marsman, M.; Kresse, G. *Phys. Rev. B* **2008**, *78*, 121201.
(69) Walsh, A.; Yan, Y.; Huda, M. N.; Al-Jassim, M. M.; Wei, S. H. *Chem. Mater.* **2009**, *21*, 547–551.
(70) Momma, K.; Izumi, F. *J. Appl. Crystallogr.* **2008**, *41*, 653–658.

Table 1. Structural Data for the GGA + *U* and HSE06 Optimized $CuBO_2$ and the Experimental Data from the Work of Snure and Tiwari[33,a]

	GGA + *U*	HSE06	experiment[33]
volume	30.76	29.42	38.46
a	2.53	2.49	2.84
c	16.58	16.43	16.52

[a] Volumes are given in Å^3 and lattice dimensions and in Å.

Table 2. Cu−O and M(III)−O Nearest-Neighbor Interatomic Distances for the GGA + *U* and HSE06 Optimized $CuBO_2$ and the Experimentally Reported Bond Lengths of $CuAlO_2$, $CuGaO_2$, and $CuInO_2$[a]

	$CuBO_2$ GGA+*U*	$CuBO_2$ HSE06	$CuAlO_2$[71]	$CuGaO_2$[71]	$CuInO_2$[72]
Cu−O	1.889	1.875	1.864	1.848	1.845
M(III)−O	1.703	1.677	1.910	1.996	2.173

[a] All interatomic distances are given in Å.

To test the validity of our prediction, the experimental trend of the *a* vector against ionic radii for some known delafossite structures is shown in Figure 2. The experimental lattice parameter reported for $CuBO_2$ is a considerable distance away from the experimental trend of the *a* lattice parameter against ionic radii. Our GGA + *U* calculated *a* value is slightly overestimated compared to the experimental trend line, as is expected from a GGA calculation, but overall is a much closer fit to the experimental trend line. The GGA + *U* results are slightly overestimated compared with the GGA+ *U* calculated lattice parameter trend for $CuAlO_2$, $CuGaO_2$, and $CuInO_2$, although this is probably a consequence of the small ionic radius of B. Minimization at the HSE06 level results in lattice parameters of $a = 2.49$ Å and $c = 16.42$ Å. The a lattice parameter from our HSE06 calculation is even closer to the experimental trend line in Figure 2. This is to be expected, as HSE06 is known to produce improved lattice parameters compared to GGA,[60] which typically overestimates by 1−2%. The HSE06 calculated *a* lattice parameters for $CuAlO_2$, $CuGaO_2$, and $CuInO_2$[73] are also displayed in Figure 2, to highlight the small deviations from the experimental trend that usually occur using this method. Similar to the GGA + *U* result, the HSE06 result for $CuBO_2$ slightly deviates from the previous HSE06 trend but is still in much greater agreement with the experimental trend than the data from Snure and Tiwari.[33] This further indicates that the *a* lattice parameter taken from the work of Snure and Tiwari is severely overestimated,[33] by as much a 0.4 Å.

The GGA + *U* calculated bandstructure of $CuBO_2$ along the high symmetry lines taken from Bradley and Cracknell[74] is shown in Figure 3. The VBM is situated at the F point, while the conduction band minimum (CBM) lies at Γ, giving an indirect band gap of 1.94 eV, with the smallest direct band gap situated at Γ and measuring 3.21 eV. This cannot be viewed as a prediction of the

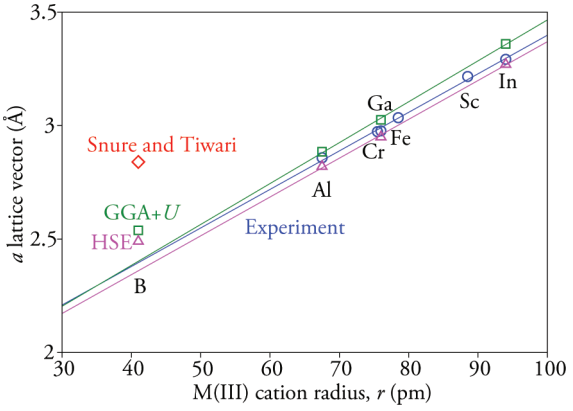

Figure 2. Plot of *a* lattice parameter versus ionic radii for some common Cu based delafossites. The blue circles signify experimental *a* lattice parameters for known delafossites,[24] the red diamond is the lattice parameter for $CuBO_2$ proposed by Snure and Tiwari,[33] the green squares signify the GGA + *U* calculated *a* lattice parameters, and the pink triangles are the HSE06 calculated *a* lattice parameters for $CuBO_2$, $CuAlO_2$, $CuGaO_2$, and $CuInO_2$.

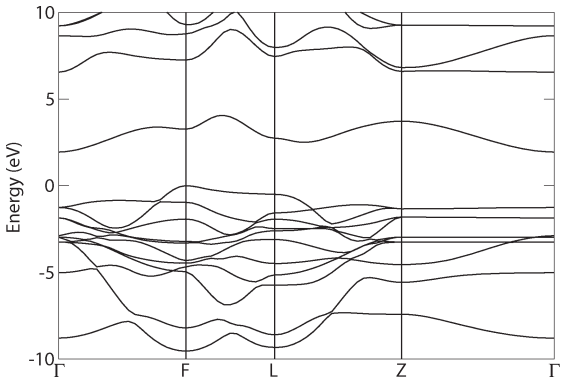

Figure 3. GGA + *U* calculated bandstructure of $CuBO_2$. The top of the valence band is set to 0 eV.

absolute value of the indirect or direct band gaps, as GGA + *U* calculations are known to produce underestimated band gaps.[43] Direct band gaps at similar energy differences are found at L (3.2 eV) and F (3.24 eV). The positioning of the VBM is a deviation from the behavior of the other group 13 delafossites predicted from LDA calculations, as $CuAlO_2$, $CuGaO_2$, and $CuInO_2$ all have VBMs situated on the line from F−Γ near F.[32]

To verify if the band gap trends observed in other group 13 delafossites are maintained, we compare the indirect and direct bandgaps for $CuBO_2$ with the previous theoretical results.[43] The other known group 13 delafossites show a trend of decreasing indirect band gap as the group 13 cation increases in atomic number, with LDA calculated indirect gaps decreasing from 1.97 eV ($CuAlO_2$) to 0.95 eV ($CuGaO_2$) to 0.43 eV ($CuInO_2$).[32] Similarly the direct band gap trends show a decrease in magnitude of the gap as the atomic number of the group 13 ion increases, with the LDA calculated direct band gaps decreasing from 2.93 eV ($CuAlO_2$) to 1.63 eV ($CuGaO_2$) to 0.73 eV ($CuInO_2$).[32] For these trends to be maintained, it would have been expected that the indirect and direct band gaps of $CuBO_2$ would be greater than those of $CuAlO_2$. As it would be remiss of us to directly compare

(71) Koehler, B. U.; Jansen, M. *Z. Kristallogr.* **1986**, *543*, 73–80.
(72) Shimode, M.; Sasaki, M.; Mukaida, K. *J. Solid State Chem.* **2000**, *151*, 16–20.
(73) Godinho, K. G.; Scanlon, D. O.; Watson, G. W. Unpublished.
(74) Bradley, C. J.; Cracknell, A. P. *Mathematical Theory of Symmetry in Solids*; Oxford Univeristy Press: New York, 1972.

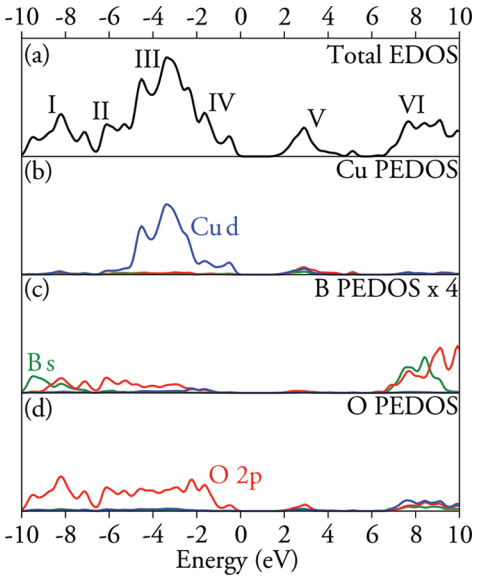

Figure 4. Electronic density of states for $CuBO_2$. (a) Total EDOS, (b) Cu PEDOS, (c) B PEDOS, and (d) O PEDOS. The blue lines represent d states, green s states, and red p states.

GGA + U band gaps to the LDA calculated bandgaps taken from the study of Wei and co-workers,[32] we instead compare with previous GGA + U results for $CuAlO_2$.[43] The indirect and direct band gaps for $CuAlO_2$ calculated at the GGA + U level are 2.2 eV and 3.1 eV, respectively.[43] As our calculated fundamental indirect band gap for $CuBO_2$ (1.94 eV) is smaller than that of $CuAlO_2$, $CuBO_2$ does not seem to follow the same trends as the other group 13 delafossites. The direct band gap however does follow the trend, with the direct band gap of $CuBO_2$ (3.21 eV) being larger than that of $CuAlO_2$ (3.1 eV).[43]

Our HSE06 calculated indirect and direct band gaps measure 3.08 eV (between F and Γ) and 3.59 eV (at F), respectively. The value of the indirect band gap is clearly larger than that reported by Snure and Tiwari[33] of 2.2 eV, and the value of the direct band gap is clearly smaller than the 4.5 eV proposed in the literature,[33] although it would be foolhardy to compare the calculated direct band gap with an optically measured band gap.[32] The HSE06 functional is expected to predict band gaps that are closer to experiment than those of LDA/GGA/GGA + U methods,[58−62] and so as large a difference as the difference reported here between experiment and calculation is unusual. This difference between the calculated indirect band gap and the experimentally measured indirect band gap, allied to the apparent anomaly in the structural data reported from the $CuBO_2$ thin films, is another indicator that an experimental reinvestigation of the structure and properties of $CuBO_2$ is warranted.

Figure 4a−d shows the calculated total and partial (ion decomposed) electronic densities of states (EDOS/PEDOS) for $CuBO_2$. The PEDOS were calculated by projecting wave functions onto atom centered spherical harmonics, with radii of 1.4 Å: for Cu, 1.1 Å for B and 1.4 Å for O. These radii reproduce the correct number of electrons in the system, and their ratios are consistent with the positions of minima observed between the atoms in valence−charge density plots. The valence band (VB) can be split up into four distinguishable regions (labeled I to IV), with the conduction band considered in two sections (V and VI).

Region I spans from −10 eV to −8 eV and is composed mainly of O 2p states, with some mixing of B s and p states. It is noticeable that the s states of B are ∼2 eV lower in energy than the s states of Al in $CuAlO_2$.[43] Region II (between −8 eV and −6.5 eV) is again dominated by O 2p states, with some minor mixing with Cu 3d and B p states. Between −6.5 eV and −2 eV (Region III), Cu 3d states dominate, with significant O 2p hybridization and some minor B p interaction. At the top of the VB, Region IV, Cu d states are dominant, as is to be expected from a Cu(I) oxide, with some mixing with O 2p states. The bottom of the CB consists of a mix of Cu 3d states and O 2p states, similar again to $CuAlO_2$.[43]

To gain a deeper understanding of the band structure features, we have plotted projections of the wave function for the VBM at F and the CBM at the Γ point through a (001) plane containing Cu, B, and O atoms, labeled (b) and (c) in Figue 5. A numerical breakdown of the states at the VBM shows that it contains ∼67% Cu d character and ∼31% oxygen p character, with B states effectively playing no role in the VBM makeup at F. This is further evidenced by the charge density plot of the VBM (Figure 5b) which clearly shows d-like orbitals on the Cu ions and p-like orbitals on the O ions, with the absence of any density on the B states. A similar numerical analysis of the CBM at Γ finds it to be composed of ∼39% Cu d, ∼21% Cu s, ∼34% O s, and only ∼5% B s. Analysis of the charge density plost of the CBM (Figure 5c) visibly shows the mixed s and d states on the Cu ions and the s-like nature of the density on the oxygen ions, with the B s states just visible.

The corresponding GGA + U and HSE06 calculated optical absorption spectra are shown in Figure 6. For $CuBO_2$, we find that fundamental band-edge transitions at the Γ and Z points are symmetry disallowed, with absorption beginning at 3.25 eV for GGA + U and 3.59 eV for HSE06. This is consistent with the findings of Nie et al., who found that the VBM and the CBM at Γ and Z have the same (even) parity for $CuMO_2$ (M = Al, Ga, In), resulting in zero dipolar optical absorption.[32] Their calculated matrix elements show that increases in the optical spectrum only occur close to the direct transition at the L and F points, which is consistent with our $CuBO_2$ results.

For the GGA + U calculated spectrum, this results in a peak centered around 5.5 eV which decreases and then subsequently ascends after 8 eV to shorter photon wavelengths. A similar pattern is seen for the HSE06 spectrum, with the peak centered at 7 eV. The HSE06 spectrum is essentially blue-shifted, with a reduction in intensity. This reduction in intensity is required by the f-sum rule.[75] The increase in width of the peak at 7 eV and the new sharper

(75) Paier, J.; Asahi, R.; Nagoya, A.; Kresse, G. *Phys. Rev. B* **2009**, *79*, 115126.

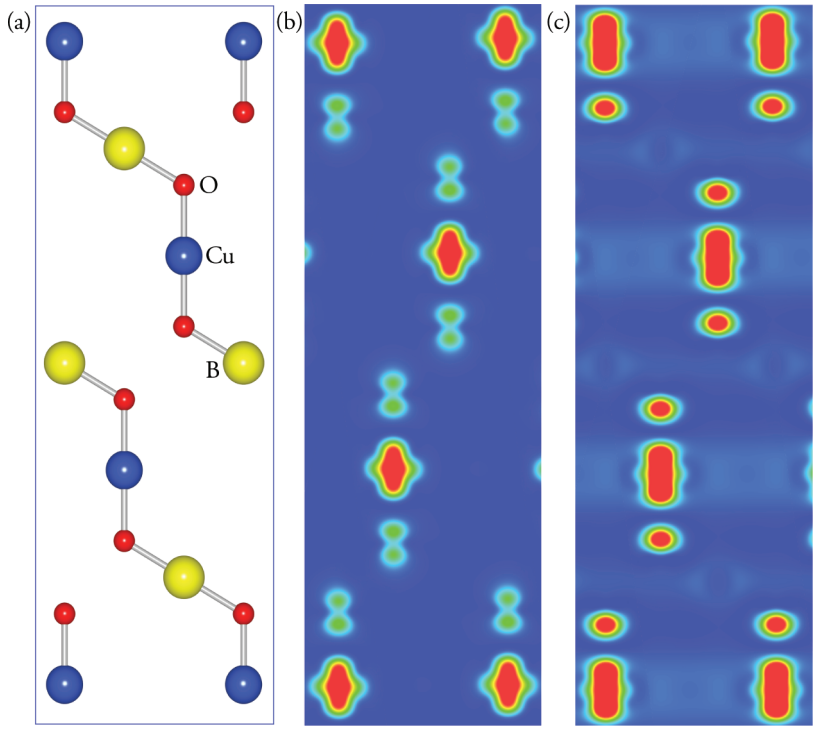

Figure 5. Charge density contour plots showing the band edges of $CuBO_2$ through a (001) plane. (a) Structure of the cell in the (001) plane, (b) charge density of the VBM at F, and (c) charge density of the CBM at Γ, plotted from 0 eV (blue) to 0.003 eV (red) e·Å^{-3}.

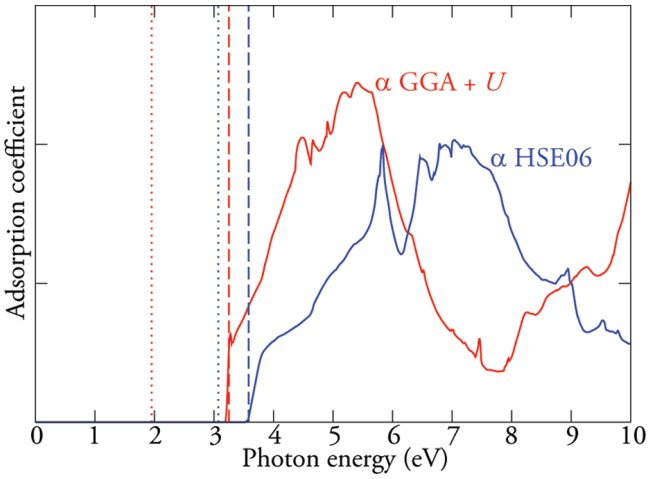

Figure 6. Calculated optical absorption spectrum of $CuBO_2$ summed over all possible direct valence to conduction band transitions. GGA + U (red) and HSE06 (blue). The dotted lines represent the fundamental indirect band gaps; the dashed lines represent the magnitude of the *optical* band gap.

peak at 6 eV are a consequence of the different effects the GGA + U and HSE06 approaches will have on individual bands.[75] These spectra show very similar features to those calculated for other group 13 delafossites ($CuMO_2$, M = Al, Ga, In) with LDA.[32] In each case the spectra featured abrupt absorption edges, although, like $CuAlO_2$ and unlike $CuGaO_2$ and $CuInO_2$, $CuBO_2$ does not have a small tail below the absorption edge. Our calculations indicate that $CuBO_2$ is indeed transparent.

In an attempt to quantify the electronic conduction properties of $CuBO_2$, we calculate the hole effective mass at the VBM and CBM. The effective mass (m^*) is calculated according to

$$\frac{1}{m^*(\mathrm{E})} = \frac{1}{\hbar^2 k}\frac{\mathrm{d}E}{\mathrm{d}k} \qquad (5)$$

where $E(k)$ is the band edge energy as a function of wave vector k, obtained directly from the GGA + U calculation.[76] In this way the diagonal elements of the effective mass tensor can be calculated for a certain k-point. Cu-based p-type TCOs are known to conduct through a polaronic hopping mechanism,[77,78] and the bands at the top of the VB are clearly not parabolic, so we do not expect $CuBO_2$ to be well described under a typical semiconductor effective mass approximation; nevertheless, the calculated effective masses serve as a rough guide of the conduction properties. At the VBM, the effective masses in the [100] and [010] directions are isotropic, measuring $1.71m_e$, with a calculated effective mass in the [001] direction of $0.45m_e$.

The effective masses of the CBM are isotropic in all three directions, with an effective mass of $1.58m_e$. Our calculated effective masses for the VBM are larger than those reported for $CuMO_2$ (M = Al, Sc, Y), but this study used the LDA functional,[79] which results in underestimated lattice parameters, smaller band gaps, and therefore lower effective masses. Recently, masses of the magnitude of $16m_e$ have been reported for the VB and

(76) Segev, D.; Wei, S. H. *Phys. Rev. B* **2005**, *71*, 125129.
(77) Ingram, B. J.; Gonzalez, G. B.; Mason, T. O.; Shahriari, D. Y.; Barnabe, A.; Ko, D.; Poeppelmeier, K. R. *Chem. Mater.* **2004**, *16*, 5616–5622.
(78) Ingram, B. J.; Harder, B. J.; Hrabe, N. W.; Mason, T. A.; Poeppelmeier, K. R. *Chem. Mater.* **2004**, *16*, 5623–5629.
(79) Shi, L. J.; Fang, Z. J.; Li, J. *J. Appl. Phys.* **2008**, *104*, 073527.

$0.24m_e$ for the CB of In_2O_3,[80] indicative of good n-type ability and bad p-type ability. This highlights that strong mixing of low binding energy cation states (here Cu d) with O 2p is required to provide valence band dispersion. Taking into account the known disproportion between the n-type ability of one of the current industry standards and the relatively bad performance of current p-type TCOs, our calculated effective masses suggest good potential for enhanced p-type performance.

Discussion

It is clear that the calculations at the GGA + U and HSE06 level bring into doubt the formation of delafossite $CuBO_2$ in the work of Snure and Tiwari.[33] Investigation of the $\Delta H_f^{CuBO_2}$ at the HSE06 level, given by

$$\mu_{Cu} + \mu_O + \mu_B = \Delta H_f^{CuBO_2} = -4.22\text{eV}$$

tells us that the material is stable with respect to dissociation. However, the material is not stable with respect to its binary oxides, Cu_2O and B_2O_3. This type of behavior has been noted previously for other multiternary compounds,[81] but this does not preclude their formation. Boron does not typically adopt octahedral coordination environments, but it has been found to be octahedrally coordinated in some ternary systems,[82] so it is not unreasonable that it could form delafossite $CuBO_2$. What is certain is that there is a pressing need for a re-examination of the crystal structure of $CuBO_2$.

At this point it is instructive to rationalize why the potential delafossite $CuBO_2$ displays better intrinsic conductivity than other Cu based TCOs. The B states do not contribute to the states that control conduction in the valence band, with the Cu d states dominating with some minor contributions from the O 2p states at the top of the VBM. In fact, it could be argued that B disrupts the VB features of the parent compound, Cu_2O, the least amount of all the M(III) cations, meaning that the p-type conduction properties are the most similar to that of Cu_2O. In such a case, the B ions simply serve to reduce the dimensionality of the system, making the band gap bigger by disrupting the three-dimensional interactions between the $3d^{10}$ electrons on neighboring Cu(I) ions in Cu_2O.[17] This view is further evidenced by the absence of any charge density on the B atoms when examining the wave functions at the VBM and CBM. This is not the case for $CuAlO_2$, $CuCrO_2$, $CuScO_2$, and $CuYO_2$ where the M(III) cation can be seen from previous calculations to play some role (however small) in the states that make up the VBM.[43,44,79,83]

The a lattice parameter could also play a key role in the higher intrinsic conductivity of $CuBO_2$ in comparison to undoped $CuAlO_2$, $CuCrO_2$, $CuYO_2$, and so forth. As conduction in delafossites is known to be governed by polaronic hopping mechanisms,[77,78] it is to be expected that the decrease in the a parameter would directly correlate to an increase in the rate of hopping. Hopping of holes from Cu to Cu has long been thought to be the p-type conduction mechanism in these materials,[84] with the distances between Cu sites being a limiting factor. With the predicted Cu−Cu distance in $CuBO_2$ being 2.49 Å and the next smallest Cu−Cu distance being in $CuAlO_2$ (2.86 Å), one can assume that the smaller Cu−Cu distance in $CuBO_2$ is responsible for its increased intrinsic conductivity. As the size of the M(III) ion increases, the Cu−Cu distances increase, presumably making hopping more difficult. Unfortunately as the size of the M(III) ion increases, so too does the ability to dope the material.[79] By this rationale, extrinsic doping of $CuBO_2$ to increase carrier concentrations and lower the Fermi level could be substantially more difficult than doping $CuInO_2$, for instance.

Many people have tried to explain the conductivity trends in p-type delafossites, through either size dependence or the effect of the M(III) ion on the system, but to date the nanoscopic conduction mechanism and trends for delafossite TCOs remains a mystery. What is certain, however, is that doping the trivalent metal site with a divalent dopant increases the conductivity significantly with an increase in hole concentration.[2]

In an attempt to explain the increasing conductivity of $CuY_{1-x}Ca_xO_2$ to $CuSc_{1-x}Mg_xO_2$ to $CuCr_{1-x}Mg_xO_2$, Nagarajan et al. postulated that the conductivity increases as the ionic radius decreases from Y−Sc−Cr.[28] This decrease in ionic radius causes a decrease in the a lattice parameter, and as a result an increased Cu d orbital overlap, leading to improved mobility. Unfortunately this size dependence theory is probably rendered invalid by the fact that the conductivity of $CuAl_{1-x}Mg_xO_2$ (4×10^{-4} S cm^{-1}) is considerably lower than that of $CuCr_{1-x}Mg_xO_2$ (220S cm^{-1}), despite the ionic radius of Al being much smaller than Cr.[24]

The effect of the M(III) ion in delafossite TCOs on the mobility of holes has also been discussed by Nagarajan and co-workers.[85] This study suggests that the lower hole mobilities in p-type delafossites (compared to Cu_2O) may be caused by the lack of Cu−O−Cu linkages as seen in Cu_2O. In the delafossite structure there are only Cu−O−M(III)−O−Cu linkages. They suggest the higher conductivities observed for $CuCrO_2$ and $CuFeO_2$ may be due to favorable mixing with the 3d states on the M(III) cation in the Cu−O−M(III)−O−Cu linkages,[85] which may lower the barrier for polaron hopping over the O−M(III)−O layers.

Conductivity in delafossite TCOs is a complex matter, with both size and electronic structure of the M(III) ion being important. It is clear that a combination of factors

(80) Walsh, A.; Da Silva, J. L. F.; Wei, S. H. *Phys. Rev. B* **2008**, *78*, 075211.
(81) Da Silva, J. L. F.; Walsh, A.; Lee, H. *Phys. Rev. B* **2008**, *78*, 224111.
(82) Eibenstein, U.; Wang, J. *J. Solid State Chem.* **1997**, *133*, 21–24.
(83) Ingram, B. J.; Mason, T. O.; Asahi, R.; Park, K. T.; Freeman, A. J. *Phys. Rev. B* **2001**, *64*, 155114.
(84) Benko, F. A.; Koffyberg, F. P. *J. Phys. Chem. Solids* **1987**, *48*, 431–443.
(85) Nagarajan, R.; Duan, N.; Jayaraj, M. K.; Li, J.; Vanaja, K. A.; Yokochi, A.; Draeseke, A.; Tate, J.; Sleight, A. W. *Int. J. Inorg. Mater.* **2001**, *3*, 265–270.

are important: (a) the M(III) ion not being too big and thus not limiting the hole hopping; (b) the M(III) ion having a favorable electronic structure, which can enhance the mobility of holes; and (c) the M(III) ion not being too small and limiting the dopability of the material. Finding a compromise between these three factors is the key and might plausibly explain why $CuCrO_2$ is currently the leading material, possessing a favorable electronic structure, and an M(III) ion big enough to allow doping and small enough to not limit hopping.

Conclusion

In this study, we have calculated the geometry and electronic structure of the delafossite TCO $CuBO_2$ using GGA + U and HSE06 density functionals. The lattice parameters reported from experiment are shown to be highly questionable, with the GGA + U and HSE06 calculated lattice parameters comparing excellently with known experimental trends. $CuBO_2$ is predicted to possess a fundamental indirect band gap of ~3.1 eV and with a predicted optical band gap of ~3.6 eV, which are an underestimation and overestimation, respectively, of previous experimental absorption data. Analysis of the band extrema shows that B plays virtually no role in the states that govern conduction. Calculated effective masses of the band edges predict good p-type conductivity, consistent with experiment. This increased intrinsic conductivity relative to other delafossite TCOs is attributed to the Cu−Cu distances in $CuBO_2$ being smaller than in any other delafossite.

Acknowledgment. G.W.W. would like to thank G. Kresse for the provision of VASP 5.1 for the HSE06 calculations. This publication has emanated from research conducted with financial support of Science Foundation Ireland: PI Grant Number 06/IN.1/I92 and 06/IN.1/I92/EC07. We also acknowledge support from the HEA for the PTRLI programs IITAC (Cycle III) and e-INIS (CYCLE IV). All calculations were performed on the IITAC supercomputer as maintained by the Trinity Centre for High Performance Computing (TCHPC) and the Stokes computer, maintained by the Irish Centre for High-End Computing (ICHEC).